# A Ligand-Exchange Mechanism of Proton Pumping Involving Tyrosine-422 of Subunit I of Cytochrome Oxidase Is Ruled Out†

David M. Mitchell,‡ Pia Ädelroth,§ Jonathan P. Hosler,||,⊥ John R. Fetter,||,# Peter Brzezinski,§ Michelle A. Pressler,○ Roland Aasa,§ Bo G. Malmström,§ James O. Alben,▽ Gerald T. Babcock,○ Robert B. Gennis,‡ and Shelagh Ferguson-Miller*,||

*School of Chemical Sciences, University of Illinois, Urbana, Illinois 61801, Departments of Biochemistry and Chemistry, Michigan State University, East Lansing, Michigan 48824, Department of Medical Biochemistry, The Ohio State University, Columbus, Ohio 43210, and Department of Biochemistry and Biophysics, Göteborg University and Chalmers University of Technology, Medicinaregatan 9C, S-413 90 Göteborg, Sweden*

*Received August 14, 1995; Revised Manuscript Received November 20, 1995*⊗

ABSTRACT: The molecular mechanism by which proton pumping is coupled to electron transfer in cytochrome *c* oxidase has not yet been determined. However, several models of this process have been proposed which are based on changes occurring in the vicinity of the redox centers of the enzyme. Recently, a model was described in which a well-conserved tyrosine residue in subunit I (Y422) was proposed to undergo ligand exchange with the histidine ligand (H419) of the high-spin heme $a_3$ during the catalytic cycle, allowing both residues to serve as part of a proton transporting system. Site-directed mutants of Y422 have been constructed in the $aa_3$-type cytochrome *c* oxidase of *Rhodobacter sphaeroides* to test this hypothesis (Y422A, Y422F). The results demonstrate that Y422 is not an essential residue in the electron transfer and proton pumping mechanisms of cytochrome *c* oxidase. However, the results support the predicted proximity of Y422 to heme $a_3$, as now confirmed by crystal structure. In addition, it is shown that the pH-dependent reversed electron transfer between heme *a* and heme $a_3$ is normal in the Y422F mutant. Hence, these data also demonstrate that Y422 is not the residue previously postulated to interact electrostatically with heme $a_3$, nor is it responsible for the unique EPR characteristics of heme *a* in this bacterial oxidase.

The mechanism of energy transduction by cytochrome *c* oxidase has been the subject of intense speculation and debate ever since Mitchell proposed that its only contribution to generation of the membrane potential in mitochondria was through asymmetric usage of matrix protons in the formation of water. In 1977, Wikström reported evidence of vectorial transport of protons by cytochrome oxidase in intact mitochondria, a finding that was confirmed with purified oxidase in reconstituted vesicles (Wikström, 1977, Wikström & Krab, 1979), ultimately leading to concurrence in the field that cytochrome oxidase is a proton pump. Nevertheless, the mechanism of this process remains obscure. A number of recent hypotheses have built on the original suggestion by Chan and co-workers (Chan & Li, 1990; Gelles et al., 1987) that a redox active metal center could accomplish vectorial proton transfer by undergoing ligand exchange during its redox cycle, accompanied by changes in protonation state of the ligands. Although the original hypothesis predicted changes in $Cu_A$ ligation, more recent ideas have focused on heme $a_3$ (Rousseau et al., 1993; Woodruff, 1993) and $Cu_B$ (Wikström et al., 1994). Rapid kinetic analysis by Woodruff and colleagues (Woodruff et al., 1991) indicates the possible loss of the histidine ligand to heme $a_3$ upon flash photolysis of CO. The heme $a_3$ proximal ligand has been identified by mutational analysis as H419 (using *Escherichia coli* and *Rhodobacter sphaeroides* numbering). (Calhoun et al., 1993; Hosler et al., 1993.) Rousseau et al. (1993) developed this idea by proposing a substitution of H419 by Y422 during normal redox cycling of the enzyme. This would allow H419 to undergo a protonation−deprotonation cycle that could drive a proton pump. Mutants of Y422, Y422F, and Y422A have been constructed in the $aa_3$-type cytochrome *c* oxidase of *R. sphaeroides* to test this hypothesis.

In addition, the Y422F mutant has been used to test another possible functional role for Y422 as regulating the pH-dependent redox equilibration between heme *a* and heme $a_3$ after flash-photolysis of the CO-bound mixed-valence enzyme, observed both in the bovine and in the bacterial enzymes (Ädelroth et al., 1995; Hallén & Brzezinski, 1994). More specifically, the rate of this reaction decreases with increasing pH, the p*K* of this transition being 8.7, and the extent increases with increasing pH. This behavior has been modeled (Ädelroth et al., 1995; Hallén et al., 1994) as an electrostatic interaction between heme $a_3$ and a protonatable group close to the binuclear center, whose p*K* shifts from

† This work was supported by NIH Grants GM-26916 (to S.F.-M.), HL-16101 (to R.B.G.), and GM-25480 (to G.T.B.), and by the Swedish Natural Science Research Council, the Commission of the European Communities, The Royal Society of Arts and Sciences in Gothenburg, and Wilhelm och Martina Lundgrens Vetenskapsfond (to B.G.M.), and by National Science Foundation Grant DMB89046145 (to J.O.A.).

* To whom correspondence should be addressed.
‡ University of Illinois.
§ Göteborg University and Chalmers University of Technology.
|| Department of Biochemistry, Michigan State University.
⊥ Current address: Department of Biochemistry, Mississippi State University Medical Center, Jackson, MS.
# Current address: Department of Biochemistry, North Carolina State University, Raleigh, NC 27695-7622.
○ Department of Chemistry, Michigan State University.
▽ The Ohio State University.

⊗ Abstract published in *Advance ACS Abstracts,* January 1, 1996.

0006-2960/96/0435-824$12.00/0 

10 to 9 upon oxidation of heme $a_3$. Potentially, Y422 would be in the appropriate range of p*K* and structural proximity to play this role; the current work tests this hypothesis.

In this paper, we report the characterization of two mutants, Y422A and Y422F, designed to test the involvement of Y422 in the electron transfer and proton pumping activity of the enzyme. The results are incompatible with an essential role for Y422 in proton pumping or in pH-dependent electron transfer, but support its predicted proximity to heme $a_3$ (Rousseau et al., 1993).

## MATERIALS AND METHODS

*Construction of Site-Directed Mutants.* Site-directed mutants were constructed using a two-step polymerase chain reaction (PCR)[1] method in which a single mutagenic oligonucleotide primer was used in conjunction with two flanking universal primers, as described by Landt et al. (1990). Vent (*exo*-) polymerase (New England Biolabs) was used for the PCR. All oligonucleotides were synthesized by the University of Illinois Biotechnology Center, Urbana, IL. The mutagenic primer sequences were as follows: Y422A, 5′-GT**T** GCG CAC TTC CAT **GC**T GTG ATG-3′; Y422F, 5′-GT**T** GCG CAC TTC CAT T**T**T GTG ATG-3′. (The mismatched base pairs are shown in boldface type.) A single *Fsp*I restriction site, **T**GCGCA, was added along with each mutation in order to facilitate screening of mutants. Introduction of this site did not affect the final amino acid sequence. The first PCR product was obtained by extension of the mutagenic primer with a single universal primer. In the second step, the first PCR product was extended in the opposite direction with a second universal primer. The final PCR product was cleaned and cut at restriction sites flanking the mutation, *Kpn*I and *Sph*I, and cloned into the plasmid pJS3 (Shapleigh et al., 1992b), a plasmid containing the entire *cta*D gene coding for subunit I of cytochrome *c* oxidase. The mutations were verified by DNA sequencing, using the Sequenase Version 2.0 DNA sequencing kit (United States Biochemical). The mutants were expressed on the plasmid pRK (Keen et al., 1988). The mutants were grown in the *R. sphaeroides* strain JS100 (Shapleigh & Gennis, 1992), a strain in which the *cta*D gene has been deleted.

*Enzyme Purification*. The purification of Y422F was facilitated by the genetic fusion of a six-histidine affinity tag to the C-terminus of subunit I, as previously described (Mitchell & Gennis, 1995). This allows the single-step purification of this mutant using a nitrilotriacetic acid−agarose affinity column. This modification has been shown previously to have no observable affect on enzyme structure of function (Mitchell & Gennis, 1995).

*Activity Assays and Spectral Measurements.* Steady-state electron transfer activity, proton pumping measurements, UV−visible spectroscopy, CO binding, and resonance Raman spectroscopy were all performed as previously described (Fetter et al., 1995; Hosler et al., 1992b, 1994). For these measurements, wild-type enzyme and the Y422 mutants were purified as described (Hosler et al., 1992b).

*Resonance Raman Spectroscopy.* Resonance Raman spectra were obtained using a Spex 1401 spectrometer equipped with a photon-counting photomultiplier detector. Excitation at 441.6 nm was provided by pumping Stilbene 420 (Coherent 599 dye laser) with multiline ultraviolet light from an argon ion laser (2W). Cytochrome *c* oxidase samples (30 $\mu$M) were reduced with sodium dithionite under $N_2$ flow and placed in capillary tubes for spectra acquisition. The spectrum was taken with 14.3 mW of power on the sample, and the average of 8 scans is shown. Temperature was maintained between 1 and 7 °C with a stream of cold $N_2$ gas.

*Fourier-Transform Infrared Spectroscopy.* Samples were prepared as previously described (Shapleigh et al., 1992a), with minor modifications. Residual water was extracted from a dithionite-reduced, CO-saturated cytoplasmic membrane preparation for a minimum of 12 h by overlaying with CO-saturated glycerol. A portion of the dehydrated sample was placed between two $CaF_2$ windows and pressed to the desired thickness. Infrared spectra were obtained with a Mattson Sirius 100 FTIR interferometer at a resolution of 0.5 $cm^{-1}$. Temperatures were maintained with a Lake Shore Cryotronics closed-cycle helium refrigerator. Spectra were obtained with a liquid $N_2$-cooled indium antimonide detector. Spectra are presented as difference spectra, in which the spectrum before photolysis (dark) is subtracted from the spectrum obtained after photolysis (light). Photodissociation was achieved by using continuous radiation from a focused 500-W tungsten bulb. Heat and UV radiation from the lamp were attenuated by passage through water and glass. Light spectra were begun after 5 min of sample illumination. Light and dark spectra are the averages of 512 scans.

*Kinetics of Internal Electron Transfers.* Mixed-valence oxidase was prepared as previously described (Brzezinski & Malmström, 1987), by an extended anaerobic incubation of oxidized enzyme in the presence of CO. The fully reduced enzyme was prepared anaerobically by adding a small excess of dithionite to the mixed-valence CO-bound enzyme. The excitation laser and observation equipment have been described in detail earlier (Hallén & Brzezinski, 1994). Kinetic traces were analyzed using a nonlinear least-squares algorithm on a personal computer.

*EPR Spectroscopy.* EPR spectra were recorded with a Bruker ER200D-SRC X-band spectrometer equipped with a standard TE102 rectangular cavity and an Oxford Instruments ESR-9 helium-flow cryostat. Experimental conditions: temperature, 10 K; microwave power, 2 mW; microwave frequency, 9.45 GHz; modulation amplitude, 2 mT; time constant, 200 ms; recording time, 100 s.

Table 1: Summary of Cytochrome *c* Oxidase Activity and Proton Pumping in Wild-Type and Mutant Enzymes

| mutant | activity (turnover) ($s^{-1}$) | proton pumping ($H^+/e^-$) |
|---|---|---|
| Y422F | 800 | 0.5−0.6 |
| Y422A | 600 | 0.5−0.6 |
| wild-type | 1200 | 0.6−0.7 |

## RESULTS

Both of the mutants, Y422F and Y422A, demonstrate substantial cytochrome oxidase activity in the purified state (45−60% of wild-type rate), and when reconstituted into artificial lipid vesicles, pump protons with efficiency similar to that of wild-type (Table 1). There are minor spectroscopic shifts in the α band of the visible spectrum (<1 nm) (not shown). The resonance Raman spectra of the mutants also show only minor effects on the heme environments (Figure 1). Most notably, the heme $a_3$ Fe−histidine stretch (214

[1] Abbreviations: PCR, polymerase chain reaction; DNA, deoxyribonucleic acid; C-terminus, carboxyl-terminus; UV, ultraviolet; FTIR, Fourier-transform infrared.

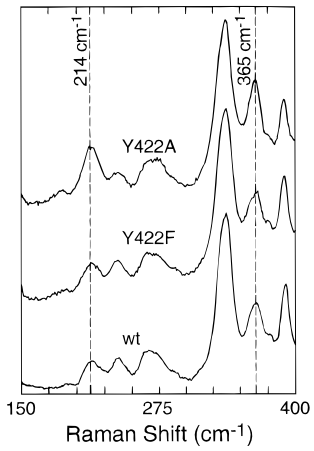


FIGURE 1: Resonance Raman spectra (low-frequency region) of the purified $aa_3$-type oxidase from *R. sphaeroides*. The wild-type (wt) spectrum is shown along with those from two mutants, Y422F and Y422A. The indicated bands at 214 and 365 $cm^{-1}$ are associated with the Fe−histidine bond. The spectra in the high-frequency region (1300−1700 $cm^{-1}$) were essentially identical for all three samples (not shown).

$cm^{-1}$) of Y422A has an increase in intensity compared to wild-type. This increased intensity of the 214 $cm^{-1}$ mode makes the low-frequency region of the Y422A RR spectrum more similar to that of bovine cytochrome *c* oxidase than to the wild-type bacterial enzyme (Babcock, 1988; Ching et al., 1985; Hosler et al., 1992b).

Low-temperature Fourier-transform (FTIR) difference spectroscopy of the reduced CO−enzyme adduct was used to probe the structure of the binuclear center in the Y422 mutants. In this method, the frequency of the CO stretch is first monitored while CO is bound to the high-spin heme $a_3$ ("dark" spectrum). After photolysis of the Fe−CO bond, CO binds to $Cu_B$, and the frequency of the CO stretch is again monitored ("light" spectrum). The "light"-minus-"dark" difference spectrum is a sensitive probe of the state of the binuclear center. The positive and negative peaks represent stretching frequencies of CO when bound to $Cu_B$ and heme $a_3$, respectively.

The FTIR difference spectra of the Y422 mutants and wild-type cytochrome *c* oxidase are shown in Figure 2. In the wild-type spectrum, two distinct frequencies are present in both the Fe−CO and Cu−CO states. Although the precise structural basis is uncertain, the two forms, α and $\beta$, appear to result from two distinct conformations of the active site of the enzyme (Fiamingo et al., 1982, 1986). The Y422A mutation, in which the bulky phenol group of tyrosine has been removed, shows only minor frequency shifts from wild-type (1 $cm^{-1}$ shifts in the Fe−CO frequencies), which rules out significant hydrogen bonding or polarization interactions between Y422 and heme $a_3$. On the other hand, Y422F, in which only the hydroxyl group of the tyrosine has been removed, shows that the $\beta$-form is favored over the α-form, implying some conformational change in the vicinity of the binuclear center.

EPR spectroscopy was also performed on the Y422F mutant (data not shown). No significant differences in spectrum of the Y422F mutant and the wild-type oxidase were observed (Hosler et al., 1992b). After incubation at low pH, a g12 signal was detectable, indicating that, despite its effects on the binuclear center environment, this mutant is able to form the self-induced slow form of the enzyme (not shown).

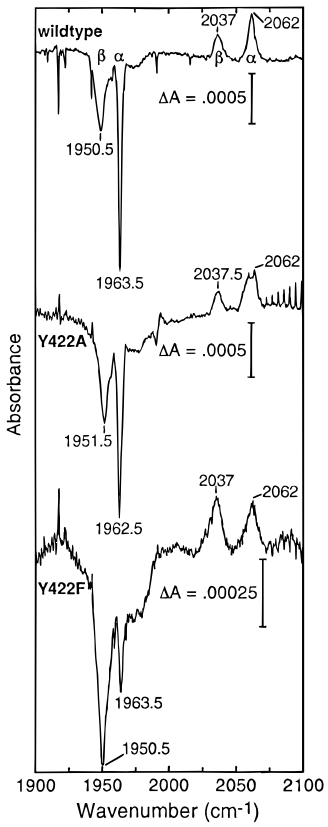


FIGURE 2: Low-temperature (30 K) FTIR difference spectra of membranes containing the wild-type $aa_3$-type oxidase, the Y422A mutant, and the Y422F mutant. Note that Y422F favors the $\beta$-form.

In order to evaluate the effect of the Y422 mutations on electron transfers within in enzyme as well as the CO recombination kinetics, absorbance changes following CO dissociation from the mixed-valence and fully reduced enzyme were followed on a microsecond to second time scale. In this method of analysis, the enzyme is in a two-electron reduced state with heme $a_3$ and $Cu_B$ of the binuclear center reduced (mixed-valence form), with CO bound to heme $a_3$ as the distal axial ligand, causing an apparent increase in the reduction potential of heme $a_3$. Upon photolysis of the Fe−CO bond, the electron is no longer stabilized on heme $a_3$ and will equilibrate with heme *a* and $Cu_A$, i.e., be transferred backward (opposite to the physiological direction) through the enzyme. This is observed as three phases in the absorbance changes following CO dissociation, where the first and second phases have been interpreted as representing transfer from heme $a_3$ to heme *a* (time constant 3 $\mu$s) and from heme *a* to $Cu_A$ (time constant 35 $\mu$s), respectively. A slower third phase (time constant around 1 ms at neutral pH) is associated with an additional transfer from heme $a_3$ to heme *a*, and has been found to be pH-dependent (Ädelroth et al., 1995; Hallén et al., 1994). The results of this analysis are presented in Table 2.

The rates and extents of electron transfers within the Y422F mutant are essentially the same as those observed in the wild-type enzyme, except for a 20% increase in the extent of the 3 $\mu$s phase for the mutant (Figure 3). The rate of CO recombination in the mixed-valence enzyme, however, is about 8 times slower in the Y422F mutant compared to the wild-type enzyme (Figure 4). The slow third phase corresponding to electron transfer from heme $a_3$ to heme *a* was measured at pH 8.8, because the extent of the reaction is close to zero at neutral pH. Both the extent and rate of this

Table 2: Internal Electron Transfer and CO Recombination Kinetics for Wild-Type and Y422F Mutant Enzymes, Measured in a Buffer Containing 0.1 M Hepes−KOH, pH 7.2, with 0.1% Dodecyl Maltoside[a]

| | wild-type | Y422F |
|---|---|---|
| (A) mixed-valence enzyme | | |
| (1) heme $a_3$ to heme $a$ | | |
| observed[b] time constant ($\mu$s) | 2.7 | 1.5 |
| extent of heme $a$ reduced (%) | 45 | 55 |
| (2) heme $a$ to $Cu_A$ | | |
| observed[b] time constant ($\mu$s) | 40 | 80 |
| extent of $Cu_A$ reduced (%) | <10 | <10 |
| (3) CO recombination | | |
| time constant[c] (ms) | 60 | 450 |
| (B) fully reduced enzyme | | |
| (1) CO recombination | | |
| time constant (ms) | 20 | 16 |

[a] The enzyme and CO concentrations were 2 $\mu$M and 1 mM, respectively. [b] The observed time constant is the inverse of the sum of the forward and backward rate constants. [c] The value is for the major phase of the reaction. In both the wild-type and Y422F mutant enzyme, there is also a small slower phase of CO recombination whose origin is not fully understood at this moment.

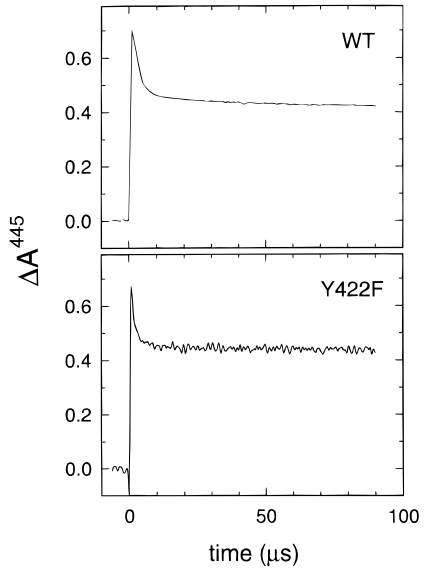


FIGURE 3: The 3-$\mu$s electron transfer from heme $a_3$ to heme $a$ in the wild-type and in the Y422F mutant cytochrome $c$ oxidase, measured at 445 nm. Conditions: 10 $\mu$M cytochrome $c$ oxidase, 100 mM Hepes at pH 7.0, 0.1% dodecyl D-maltoside, and 1 mM CO. The temperature was 21 ± 1 °C.

reaction were found to be the same as those with wild-type enzyme at the same pH (Figure 5).

## DISCUSSION

The residue at position 422 is one helix turn below H419, the heme $a_3$ proximal ligand (Calhoun et al., 1993; Hosler et al., 1993), and next to H421, one of the two heme $a$ ligands (Lemieux et al., 1992; Shapleigh et al., 1992b). This central location and its moderately high degree of conservation make it potentially interesting from a structural and functional perspective. Y422 has been proposed to facilitate electron transfer between heme $a$ and heme $a_3$ (Brown et al., 1993). The idea of direct participation of Y422 in a proton pump was a provocative suggestion (Rousseau et al., 1993), and inspired the work described in the current investigation. The data definitively demonstrate the following: (1) Y422 is not required for oxidase electron transfer or proton pumping functions. (2) Y422 cannot be a substitute axial ligand to

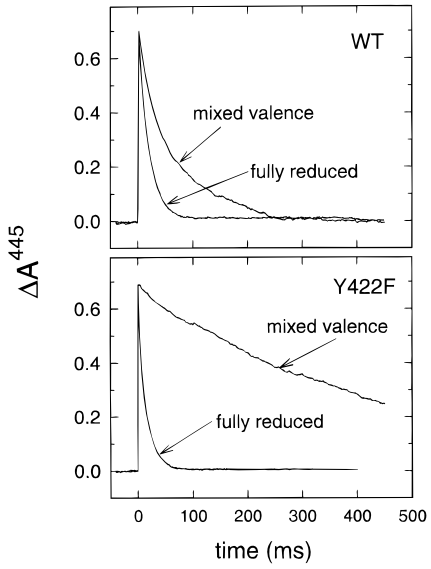


FIGURE 4: Comparison of the CO recombination kinetics in mixed-valence and fully reduced wild-type (wt) and Y422F mutant cytochrome $c$ oxidase measured at 445 nm. The experimental conditions were the same as in Figure 3.

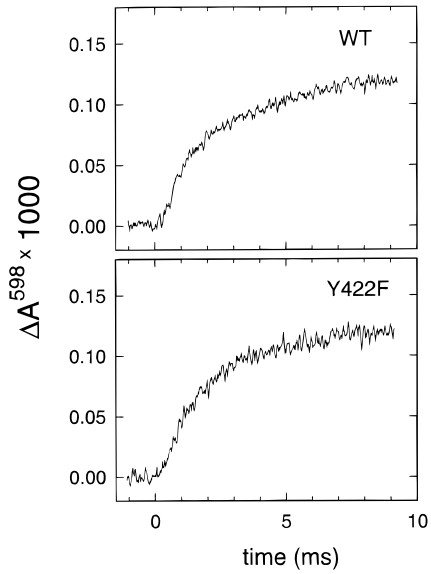


FIGURE 5: The millisecond (third phase) electron transfer from heme $a_3$ to heme $a$ in wild-type and Y422F mutant cytochrome $c$ oxidase, measured at ~598 nm (isosbestic point for the CO dissociation). A small remaining CO dissociation absorbance change has been truncated in the lower trace for easier comparison of the two traces. Conditions were the same as in Figure 3 except that the buffer was 100 mM Tris at pH 8.8.

heme $a_3$ as proposed (Rousseau et al., 1993). (3) Y422 is not the residue responsible for the pH dependence of the electron equilibration between heme $a$ and heme $a_3$ (Hallén et al., 1994). However, as discussed below, the data do reveal some interesting spectral and kinetic characteristics of mutants at this position, and confirm the location near heme $a_3$.

Visible and resonance Raman analysis of Y422F suggests that the aromatic character of phenylalanine at position 422 is sufficient to maintain normal structure around each of the heme centers. However, low-temperature FTIR reveals a shift toward the $\beta$-forms of the CO adducts of heme $a_3$ and $Cu_B$ in Y422F. The $\beta$-forms may result from a more relaxed conformer of the heme $a_3$−$Cu_B$ pocket (Wang et al., 1995). Both the FTIR result and the fact that CO recombination in

Y422F is slowed (see below) suggest a subtle effect of the Y422F mutation on the binuclear center.

The rates and extents of electron transfers in the Y422F mutant are similar to those of the wild-type enzyme, except for a 20% increase in the extent of the 3 $\mu$s phase, presumably due to a somewhat smaller difference between the reduction potentials of heme $a_3$ and heme $a$ in the mutant enzyme (Table 2).

The most surprising feature in the flash-photolysis study is the very slow CO recombination in the mixed-valence form of Y422F (450 ms) compared to the wild-type enzyme (60 ms). In the fully reduced enzyme, the CO recombination time constants are essentially the same (about 20 ms).

The CO recombination rate in the mixed-valence enzyme is dependent on the extent of reduction of heme $a_3$, since CO binds only to the fraction of enzyme molecules with heme $a_3$ reduced:

$$x^- \; a_3^{3+} \xrightarrow[\text{rapid}]{} x a_3^{2+} \xrightarrow[\text{slow}]{+CO} x a_3^{2+}\cdot CO$$

Assuming the simplest model possible, the observed CO recombination rate is given by

$$k_{obs} = k_{co}\frac{[a_3^{2+}]}{[a_3^{2+}] + [a_3^{3+}]} \qquad (1)$$

where $k_{co}$ is the CO recombination rate for the fully reduced enzyme. The large difference in CO recombination rate for the mixed-valence enzyme (450 *vs* 60 ms for the wild-type) cannot be explained in terms of the slight increase in the extent of the electron backflow for the Y422F mutant (55% *vs* 45% for the wild-type). If the extent of reduction of heme $a_3$ were limiting, this would imply that heme $a_3$ is oxidized to 96% following CO dissociation, which is not observed. Hence, the simple model above cannot explain the very slow CO recombination observed with the Y422F mixed-valence enzyme. Instead the data suggest that the Y422F mutation specifically affects reactions following CO dissociation in the mixed-valence enzyme, e.g., if $Cu_B$ becomes (partly) oxidized or structural changes occur upon oxidation of heme $a_3$ limiting the rate of CO recombination (Woodruff, 1993). When the enzyme is fully reduced, the FTIR spectrum (Figure 2) demonstrates that the Y422F mutation does alter the conformation at the binuclear center. However, this does not result in any alteration of the CO recombination rate with the fully reduced enzyme.

Overall the data confirm that Y422 is in proximity to the binuclear center, completely consistent with the recently published crystal structure of the homologous *Paracoccus denitrificans* cytochrome oxidase (Iwata et al., 1995). The possibility that this tyrosine serves as the proton-donating ligand proposed to play a role in the slowest pH-dependent electron transfer reaction (Hallén et al., 1994) is ruled out since this phase is the same in the mutant as in the wild-type enzyme. Similarly, Y422 cannot function as an alternate axial ligand to heme $a_3$ and is not essential for proton pumping (Rousseau et al., 1993). It is concluded that Y422 does not have a specific role in oxidase function.

## REFERENCES


Ädelroth, P., Brzezinski, P., & Malmström, B. G. (1995) *Biochemistry 34*, 2844−2849.

Babcock, G. T. (1988) in *Biological Applications of Raman Spectroscopy* (Spiro, T. G., Ed.) J. Wiley and Sons, New York.

Brown, S., Moody, A. J., Mitchell, R., & Rich, P. R. (1993) *FEBS Lett. 316*, 216−223.

Brzezinski, P., & Malmström, B. G. (1987) *Biochim. Biophys. Acta 894*, 29−38.

Calhoun, M. W., Thomas, J. W., Hill, J. J., Hosler, J. P., Shapleigh, J. P., Tecklenburg, M. M. J., Ferguson-Miller, S., Babcock, G. T., Alben, J. O., & Gennis, R. B. (1993) *Biochemistry 32*, 10905−10911.

Chan, S. I., & Li, P. M. (1990) *Biochemistry 29*, 1−12.

Ching, Y., Argade, P. V., & Rousseau, D. L. (1985) *Biochemistry 24*, 4938−4946.

Fetter, J. R., Qian, J., Shapleigh, J., Thomas, J. W., Garcia-Horsman, A., Schmidt, E., Hosler, J., Babcock, G. T., Gennis, R. B., & Ferguson-Miller, S. (1995) *Proc. Natl. Acad. Sci. U.S.A. 92*, 1604−1608.

Fiamingo, F. G., Altschuld, R. A., Moh, P. P., & Alben, J. O. (1982) *J. Biol. Chem. 257*, 1639−1650.

Fiamingo, F. G., Altschuld, R. A., & Alben, J. O. (1986) *J. Biol. Chem. 261*, 12976−12987.

Gelles, J., Blair, D. F., & Chan, S. I. (1987) *Biochim. Biophys. Acta 853*, 205−236.

Hallén, S., & Brzezinski, P. (1994) *Biochim. Biophys. Acta 1184*, 207−218.

Hallén, S., Brzezinski, P., & Malmström, B. G. (1994) *Biochemistry 33*, 1467−1472.

Hosler, J., Fetter, J., Shapleigh, J., Espe, M., Thomas, J., Kim, Y., Gennis, R., Babcock, G., & Ferguson-Miller, S. (1992a) *EBEC 7*, 38.

Hosler, J. P., Fetter, J., Tecklenberg, M. M. J., Espe, M., Lerma, C., & Ferguson-Miller, S. (1992b) *J. Biol. Chem. 267*, 24264−24272.

Hosler, J. P., Ferguson-Miller, S., Calhoun, M. W., Thomas, J. W., Hill, J., Lemieux, L., Ma, J., Georgiou, C., Fetter, J., Shapleigh, J., Tecklenburg, M. M. J., Babcock, G. T., & Gennis, R. B. (1993) *J. Bioenerg. Biomembr. 25*, 121−136.

Hosler, J. P., Shapleigh, J. P., Tecklenburg, M. M. J., Thomas, J. W., Kim, Y., Espe, M., Fetter, J., Babcock, G. T., Alben, J. O., Gennis, R. B., & Ferguson-Miller, S. (1994) *Biochemistry 33*, 1194−1201.

Iwata, S., Ostermeier, C., Ludwig, B., & Michel, H. (1995) *Nature 376*, 660−669.

Keen, N. T., Tamaki, S., Kobayashi, D., & Trollinger, D. (1988) *Gene 70*, 191−197.

Landt, O., Grunert, H.-P., & Hahn, U. (1990) *Gene 96*, 125−128.

Lemieux, L. J., Calhoun, M. W., Thomas, J. W., Ingledew, W. J., & Gennis, R. B. (1992) *J. Biol. Chem. 267*, 2105−2113.

Mitchell, D. M., & Gennis, R. B. (1995) *FEBS Lett. 368*, 148−150.

Rousseau, D. L., Ching, Y., & Wang, J. (1993) *J. Bioenerg. Biomembr. 25*, 165−176.

Shapleigh, J. P., & Gennis, R. B. (1992) *Mol. Microbiol. 6*, 635−642.

Shapleigh, J. P., Hill, J. J., Alben, J. O., & Gennis, R. B. (1992a) *J. Bacteriol. 174*, 2338−2343.

Shapleigh, J. P., Hosler, J. P., Tecklenburg, M. M. J., Kim, Y., Babcock, G. T., Gennis, R. B., & Ferguson-Miller, S. (1992b) *Proc. Natl. Acad. Sci. U.S.A. 89*, 4786−4790.

Wang, J., Takahashi, S., Rousseau, D. L., Hosler, J. P., Ferguson-Miller, S., Mitchell, D. M., & Gennis, R. B. (1995) *Biochemistry 34*, 9819−9825.

Wikström, M. (1977) *Nature 266*, 271−273.

Wikström, M., & Krab, K. (1979) *Biochim. Biophys. Acta 549*, 177−222.

Wikström, M., Bogachev, A., Finel, M., Morgan, J. E., Puustinen, A., Raitio, M., Verkhovskaya, M., & Verkhovsky, M. I. (1949) *Biochim. Biophys. Acta 1187*, 106−111.

Woodruff, W. H. (1993) *J. Bioenerg. Biomembr. 25*, 177−188.

Woodruff, W. H., Einarsdottir, O., Dyer, R. B., Bagley, K. A., Palmer, G., Atherton, S. J., Goldbeck, R. A., Dawes, T. D., & Kliger, D. S. (1991) *Proc. Natl. Acad. Sci. U.S.A. 88*, 2588−2592.


BI951897T